Applying *LabRGB* to Real Multi-Spectral Images

Fumio Nakaya and Noboru Ohta, Fuji Xerox Co., Ltd., Kanagawa, Japan

Abstract

A spectral encoding/decoding method, called LabRGB, was proposed last year [1]. LabRGB consists of six unique base functions and physically meaningful encoding values. LabRGB has several features; color characteristics can be estimated by its encoding values, fixed base functions need not exchange beforehand and tri-chromatic images as well as multi-spectral images can be handled by a single form. In this paper, the derivation of LabRGB was described in detail including fast straightforward calculation of encoding/decoding calculation. Then LabRGB was applied to real multi-spectral images. LabRGB performed well in encoding/decoding various types of multi-spectral images and confirmed to be suitable for practical use.

Introduction

Spectral encoding/decoding using eigenvectors is a well-known method since a long time ago. Generally speaking, it shows the least estimation error. On the other hand, eigenvectors cannot be defined uniquely, because they depend on a sample selection of population. Also, encoding/decoding values using eigenvectors have no physical meaning. So it is difficult to directly estimate either a shape of spectral reflectance, or color characteristics of an original object color. It is therefore not easy to verify an encoding / decoding process. Furthermore, it cannot be applied to current tri-chromatic imaging systems directly. As such, several challenges have been made on an encoding/decoding method described above. A recently reported one is *LabPQR* [2]. *LabPQR* is a concept of the encoding which has three dimensions (*CIELAB* [3]) to represent the colorimetric characteristics of a color under a specific illuminant and additional dimensions (*PQR*) to describe the metameric black spectrum of a spectral power distribution [4]. The intention of *LabPQR* is to convey physical values so that an encoding value can be used to estimate an original object color. Several variations of the *PQR* aspects of *LabPQR* have been described in the literature [2], [5] including those based on a population of samples or those based on fundamental spectral stimuli4. Aforementioned *LabRGB* is another variation of the *LabPQR* concept. *LabRGB* has unique, well-defined base functions, physically meaningful encoding values, and are cable of handling both spectral imaging and current tri-chromatic imaging equipments. *LabRGB* encoding/decoding process has been described in the previous paper [1].

LabRGB encoding/decoding is done with the following way. The base functions set chosen as shown in Eq. 1. The first three base functions are roughly designed to represent *RGB* spectral distribution curve and the last three base functions cover higher frequency.

$$\left.\begin{aligned}
e_1(\lambda) &= \sin\left(\frac{1}{2}\pi\frac{\lambda-\lambda_{\min}}{\lambda_{\max}-\lambda_{\min}}\right)\\
e_2(\lambda) &= \cos\left(\frac{1}{2}\pi\frac{\lambda-\lambda_{\min}}{\lambda_{\max}-\lambda_{\min}}\right)\\
e_3(\lambda) &= \sin\left(\pi\frac{\lambda-\lambda_{\min}}{\lambda_{\max}-\lambda_{\min}}\right)\\
e_4(\lambda) &= \cos\left(\frac{3}{2}\pi\frac{\lambda-\lambda_{\min}}{\lambda_{\max}-\lambda_{\min}}\right)\\
e_5(\lambda) &= \sin\left(2\pi\frac{\lambda-\lambda_{\min}}{\lambda_{\max}-\lambda_{\min}}\right)\\
e_6(\lambda) &= \cos\left(\frac{5}{2}\pi\frac{\lambda}{\lambda_{\max}-\lambda_{\min}}\right)
\end{aligned}\right\} \tag{1}$$

With this base functions set, color characteristics can be estimated by weighting factors of the six base functions. The shape of the trigonometric base functions are shown in Fig. 1.

Spectral reflectance estimation was made using an equation obtained by substituting Eq. 1 into the following Eq. 2.

$$\hat{\rho}(\lambda) = \sum_{i=1}^{6} w_i \cdot e_i(\lambda) \tag{2}$$

Where, λ is wavelength, $\hat{\rho}(\lambda)$ is spectral reflectance estimation of an object color, $e_i(\lambda)$ is i-th base function and, w_i is a weighting factor of the i-th base function.

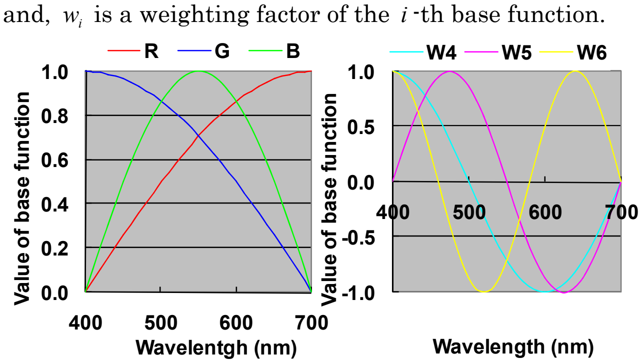

Figure 1. LabRGB base function

LabRGB uses a combination of *CIELAB* and *RGB*. Encoding is done by the following steps.

a) Calculate *CIEXYZ* and *CIELAB* [6] values of spectral reflectance of an object color $\rho(\lambda)$ using CIE1931 2 degree observer

b) Substitute Eq. 1 and $\rho(\lambda)$ into Eq. 2 and calculate 6 weighting factors $w_1 \sim w_6$ for 6 base functions by multiple regression analysis

The actual LabRGB encoding values are $L^*\ a^*\ b^*\ w_1\ w_2\ w_3$.

Decoding is done by the following steps.

a) Calculate an estimation of *CIEXYZ* values $\hat{X}\hat{Y}\hat{Z}$ using only $w_1\ w_2\ w_3$ as,

$$\left.\begin{aligned}\hat{X} &= \sum_{i=1}^{3} w_i \int e_i(\lambda)\cdot E(\lambda)\cdot \bar{x}(\lambda)d\lambda \\ \hat{Y} &= \sum_{i=1}^{3} w_i \int e_i(\lambda)\cdot E(\lambda)\cdot \bar{y}(\lambda)d\lambda \\ \hat{Z} &= \sum_{i=1}^{3} w_i \int e_i(\lambda)\cdot E(\lambda)\cdot \bar{z}(\lambda)d\lambda\end{aligned}\right\} \tag{3}$$

b) Calculate *XYZ* values from the first three *LabRGB* encoding values $L^*\ a^*\ b^*$, then calculate $w_4\ w_5\ w_6$ from *XYZ* values and estimated $\hat{X}\hat{Y}\hat{Z}$ values using Eq. 4 by solving three dimensional 1st order equation

$$\left.\begin{aligned}X-\hat{X} &= \sum_{i=4}^{6} w_i \int e_i(\lambda)\cdot E(\lambda)\cdot \bar{x}(\lambda)d\lambda \\ Y-\hat{Y} &= \sum_{i=4}^{6} w_i \int e_i(\lambda)\cdot E(\lambda)\cdot \bar{y}(\lambda)d\lambda \\ Z-\hat{Z} &= \sum_{i=4}^{6} w_i \int e_i(\lambda)\cdot E(\lambda)\cdot \bar{z}(\lambda)d\lambda\end{aligned}\right\} \tag{4}$$

c) Substituting obtained $w_4\ w_5\ w_6$ and the three encoding values $w_1\ w_2\ w_3$ into Eq. 2 to calculate spectral reflectance estimation of an object color $\hat{\rho}(\lambda)$

LabRGB showed almost equal performance to traditional orthogonal eigenvector method in spectral estimation, and even better performance in colorimetric estimation.

The current LabRGB involves multiple regression calculation in encoding process and three dimensional 1st order equations in its decoding process. These two calculations involved fair amount of computation time.

This paper describes the derivation of fast straightforward *LabRGB* calculation and the results of applying *LabRGB* to real multi-spectral images.

Straightforward encoding by multiple regression coefficients

Residual error of a spectral reflectance curve D can be written as Eq. 5, where, $\rho(\lambda)$ is spectral reflectance of an object color and $\hat{\rho}(\lambda)$ is spectral reflectance estimation of an object color.

$$D = \int \sum_{i=1}^{6} \{\hat{\rho}(\lambda) - \rho(\lambda)\}^2 d\lambda \tag{5}$$

The best estimation condition is given by Eq. 6.

$$\frac{\partial D}{\partial w_i} = 0 \tag{6}$$

Equation 7 is obtained by substituting Eq. 5 into Eq.6 and implementing partial differentiation.

$$\int e_i(\lambda)\{\sum_{i=1}^{6} w_i \cdot e_i(\lambda) - \rho(\lambda)\}d\lambda = 0 \tag{7}$$

Eq. 7 can be written as Eq. 8.

$$\int e_i(\lambda)\{\sum_{i=1}^{6} w_i \cdot e_i(\lambda)\}d\lambda = \int e_i(\lambda)\rho(\lambda)d\lambda = b_i \tag{8}$$

Matrix expression of Eq. 8 is obtained by Eq. 9.

$$\begin{pmatrix} E_1\cdot E_1 & E_1\cdot E_2 & E_1\cdot E_3 & E_1\cdot E_4 & E_1\cdot E_5 & E_1\cdot E_6 \\ E_2\cdot E_1 & E_2\cdot E_2 & E_2\cdot E_3 & E_2\cdot E_4 & E_2\cdot E_5 & E_2\cdot E_6 \\ E_3\cdot E_1 & E_3\cdot E_2 & E_3\cdot E_3 & E_3\cdot E_4 & E_3\cdot E_5 & E_3\cdot E_6 \\ E_4\cdot E_1 & E_4\cdot E_2 & E_4\cdot E_3 & E_4\cdot E_4 & E_4\cdot E_5 & E_4\cdot E_6 \\ E_5\cdot E_1 & E_5\cdot E_2 & E_5\cdot E_3 & E_5\cdot E_4 & E_5\cdot E_5 & E_5\cdot E_6 \\ E_6\cdot E_1 & E_6\cdot E_2 & E_6\cdot E_3 & E_6\cdot E_4 & E_6\cdot E_5 & E_6\cdot E_6 \end{pmatrix} \bullet \begin{pmatrix} w_1 \\ w_2 \\ w_3 \\ w_4 \\ w_5 \\ w_6 \end{pmatrix} = \begin{pmatrix} b_1 \\ b_2 \\ b_3 \\ b_4 \\ b_5 \\ b_6 \end{pmatrix} \tag{9}$$

where, b_i are constant when spectral reflectance of an object color $\rho(\lambda)$ was given.

For simplicity, modify Eq. 1 as Eq. 10.

$$\left.\begin{aligned} &E_1 = \sin\left(\frac{1}{2}\pi x\right),\ E_2 = \cos\left(\frac{1}{2}\pi x\right),\ E_3 = \sin(\pi x) \\ &E_4 = \cos\left(\frac{3}{2}\pi x\right),\ E_5 = \sin(2\pi x),\ E_6 = \cos\left(\frac{5}{2}\pi x\right)\end{aligned}\right\} \tag{10}$$

where, $0 \le x \le 1$

The each element of left hand side of matrix in Eq. 10 can be calculated in the following manner.

$$E_1\cdot E_1 = \int_0^{\frac{\pi}{2}} \sin(x)\sin(x)dx\ ,\ E_1\cdot E_2 = \int_0^{\frac{\pi}{2}} \sin(x)\cos(x)dx\cdot\cdot$$

$$E_1\cdot E_3 = \int_0^{\frac{\pi}{2}} \sin(x)\sin(2x)dx\cdot,\ E_1\cdot E_4 = \int_0^{\frac{\pi}{2}} \sin(x)\cos(3x)dx$$

$$E_1\cdot E_5 = \int_0^{\frac{\pi}{2}} \sin(x)\sin(4x)dx\ ,\ E_1\cdot E_6 = \int_0^{\frac{\pi}{2}} \sin(x)\cos(5x)dx\cdot$$

$$E_2\cdot E_1 = \int_0^{\frac{\pi}{2}} \cos(x)\sin(x)dx\ ,\ E_2\cdot E_2 = \int_0^{\frac{\pi}{2}} \cos(x)\cos(x)dx$$

$$E_2\cdot E_3 = \int_0^{\frac{\pi}{2}} \cos(x)\sin(2x)dx\ ,\ E_2\cdot E_4 = \int_0^{\frac{\pi}{2}} \cos(x)\cos(3x)dx$$

$$E_2\cdot E_5 = \int_0^{\frac{\pi}{2}} \cos(x)\sin(4x)dx\ ,\ E_2\cdot E_6 = \int_0^{\frac{\pi}{2}} \cos(x)\cos(5x)dx$$

$$E_3\cdot E_1 = \int_0^{\frac{\pi}{2}} \sin(2x)\sin(x)dx\ ,\ E_3\cdot E_2 = \int_0^{\frac{\pi}{2}} \sin(2x)\cos(x)dx$$

$$E_3\cdot E_3 = \int_0^{\frac{\pi}{2}} \sin(2x)\sin(2x)dx\ ,\ E_3\cdot E_4 = \int_0^{\frac{\pi}{2}} \sin(2x)\cos(3x)dx$$

$$E_3\cdot E_5 = \int_0^{\frac{\pi}{2}} \sin(2x)\sin(4x)dx\ ,\ E_3\cdot E_6 = \int_0^{\frac{\pi}{2}} \sin(2x)\cos(5x)dx$$

$$E_4\cdot E_1 = \int_0^{\frac{\pi}{2}} \cos(3x)\sin(x)dx\ ,\ E_4\cdot E_2 = \int_0^{\frac{\pi}{2}} \cos(3x)\cos(x)dx$$

$$E_4 \cdot E_3 = \int_0^{\frac{\pi}{2}} \cos(3x)\sin(2x)dx\,,\ E_4 \cdot E_4 = \int_0^{\frac{\pi}{2}} \cos(3x)\cos(3x)dx$$

$$E_4 \cdot E_5 = \int_0^{\frac{\pi}{2}} \cos(3x)\sin(4x)dx\,,\ E_4 \cdot E_6 = \int_0^{\frac{\pi}{2}} \cos(3x)\cos(5x)dx$$

$$E_5 \cdot E_1 = \int_0^{\frac{\pi}{2}} \sin(4x)\sin(x)dx\,,\ E_5 \cdot E_2 = \int_0^{\frac{\pi}{2}} \sin(4x)\cos(x)dx$$

$$E_5 \cdot E_3 = \int_0^{\frac{\pi}{2}} \sin(4x)\sin(2x)dx\,,\ E_5 \cdot E_4 = \int_0^{\frac{\pi}{2}} \sin(4x)\cos(3x)dx$$

$$E_5 \cdot E_5 = \int_0^{\frac{\pi}{2}} \sin(4x)\sin(4x)dx\,,\ E_5 \cdot E_6 = \int_0^{\frac{\pi}{2}} \sin(4x)\cos(5x)dx$$

$$E_6 \cdot E_1 = \int_0^{\frac{\pi}{2}} \cos(5x)\sin(x)dx\,,\ E_6 \cdot E_2 = \int_0^{\frac{\pi}{2}} \cos(5x)\cos(x)dx$$

$$E_6 \cdot E_3 = \int_0^{\frac{\pi}{2}} \cos(5x)\sin(2x)dx\,,\ E_6 \cdot E_4 = \int_0^{\frac{\pi}{2}} \cos(5x)\cos(3x)dx$$

$$E_6 \cdot E_5 = \int_0^{\frac{\pi}{2}} \cos(5x)\sin(4x)dx\,,\ E_6 \cdot E_6 = \int_0^{\frac{\pi}{2}} \cos(5x)\cos(5x)dx$$

Therefore Eq. 9 can be re-written as Eq. 11.

$$\begin{pmatrix} \pi/4 & 1/2 & 2/3 & -1/2 & -4/15 & 1/6 \\ 1/2 & \pi/4 & 2/3 & 0 & -4/15 & 0 \\ 2/3 & 2/3 & \pi/4 & -2/5 & 0 & 2/21 \\ -1/2 & 0 & -2/5 & \pi/4 & 4/7 & 0 \\ -4/15 & -4/15 & 0 & 4/7 & \pi/4 & 4/9 \\ 1/6 & 0 & 2/21 & 0 & 4/9 & \pi/4 \end{pmatrix} \bullet \begin{pmatrix} w_1 \\ w_2 \\ w_3 \\ w_4 \\ w_5 \\ w_6 \end{pmatrix} = \begin{pmatrix} b_1 \\ b_2 \\ b_3 \\ b_4 \\ b_5 \\ b_6 \end{pmatrix} \tag{11}$$

Then, 6 weighting factors $w_1 \sim w_6$ are obtained by Eq. 12.

$$\begin{pmatrix} w_1 \\ w_2 \\ w_3 \\ w_4 \\ w_5 \\ w_6 \end{pmatrix} = \begin{pmatrix} \pi/4 & 1/2 & 2/3 & -1/2 & -4/15 & 1/6 \\ 1/2 & \pi/4 & 2/3 & 0 & -4/15 & 0 \\ 2/3 & 2/3 & \pi/4 & -2/5 & 0 & 2/21 \\ -1/2 & 0 & -2/5 & \pi/4 & 4/7 & 0 \\ -4/15 & -4/15 & 0 & 4/7 & \pi/4 & 4/9 \\ 1/6 & 0 & 2/21 & 0 & 4/9 & \pi/4 \end{pmatrix}^{-1} \bullet \begin{pmatrix} b_1 \\ b_2 \\ b_3 \\ b_4 \\ b_5 \\ b_6 \end{pmatrix} \tag{12}$$

The Straightforward calculation of multiple regression coefficients is given by Eq. 13.

$$\begin{pmatrix} w_1 \\ w_2 \\ w_3 \\ w_4 \\ w_5 \\ w_6 \end{pmatrix} = \begin{pmatrix} 0.45727 & -4.9302 & 6.6638 & 5.8619 & -2.9898 & -0.97809 \\ -4.9302 & 580.18 & -811.41 & -655.31 & 327.70 & 87.578 \\ 6.6638 & -811.41 & 1135.4 & 917.16 & -459.05 & -122.80 \\ 5.8619 & -655.31 & 917.16 & 742.27 & -372.25 & -100.13 \\ -2.9898 & 327.70 & 459.05 & -372.25 & 187.33 & 50.719 \\ -0.97809 & 87.578 & -122.80 & -100.13 & 50.719 & 14.021 \end{pmatrix}^{-1} \bullet \begin{pmatrix} b_1 \\ b_2 \\ b_3 \\ b_4 \\ b_5 \\ b_6 \end{pmatrix} \tag{13}$$

Straightforward decoding by three dimensional 1st order equations

The matrix expression of Eq. 4 is given by Eq. 14,

$$\begin{pmatrix} X - \hat{X} \\ Y - \hat{Y} \\ Z - \hat{Z} \end{pmatrix} = \begin{pmatrix} Sx_4 & Sx_5 & Sx_6 \\ Sy_4 & Sy_5 & Sy_6 \\ Sz_4 & Sz_5 & Sz_6 \end{pmatrix} \bullet \begin{pmatrix} w_4 \\ w_5 \\ w_6 \end{pmatrix} \tag{14}$$

where,

$$Sx_i = \int e_i(\lambda) \cdot E(\lambda) \cdot \bar{x}(\lambda) d\lambda$$
$$Sy_i = \int e_i(\lambda) \cdot E(\lambda) \cdot \bar{y}(\lambda) d\lambda$$
$$Sz_i = \int e_i(\lambda) \cdot E(\lambda) \cdot \bar{z}(\lambda) d\lambda$$

(i=4, 5, 6)

3 weighting factors $w_4\ w_5\ w_6$ are obtained by Eq. 15.

$$\begin{pmatrix} w_4 \\ w_5 \\ w_6 \end{pmatrix} = \begin{pmatrix} S_4 & S_5 & S_6 \\ S_4 & S_5 & S_6 \\ S_4 & S_5 & S_6 \end{pmatrix}^{-1} \bullet \begin{pmatrix} X - \hat{X} \\ Y - \hat{Y} \\ Z - \hat{Z} \end{pmatrix} \tag{15}$$

Above S_i is a function of illuminant. So, the matrices for D65, D50 and BBR4K (black body radiation of 4000K) are shown bellow.

$$\begin{pmatrix} S_4 & S_5 & S_6 \\ S_4 & S_5 & S_6 \\ S_4 & S_5 & S_6 \end{pmatrix}_{D65}^{-1} = \begin{pmatrix} -0.01262 & -0.01118 & -0.00600 \\ 0.00628 & 0.00990 & 0.01473 \\ 0.02250 & -0.01186 & 0.00740 \end{pmatrix}$$

$$\begin{pmatrix} S_4 & S_5 & S_6 \\ S_4 & S_5 & S_6 \\ S_4 & S_5 & S_6 \end{pmatrix}_{D50}^{-1} = \begin{pmatrix} -0.01063 & -0.01158 & -0.00914 \\ 0.00566 & 0.00921 & 0.00202 \\ 0.02169 & -0.01298 & 0.01101 \end{pmatrix}$$

$$\begin{pmatrix} S_4 & S_5 & S_6 \\ S_4 & S_5 & S_6 \\ S_4 & S_5 & S_6 \end{pmatrix}_{BBR4K}^{-1} = \begin{pmatrix} -0.00777 & -0.01330 & -0.01298 \\ 0.00376 & 0.01049 & 0.02692 \\ 0.02028 & -0.01317 & 0.01518 \end{pmatrix}$$

Spectral encoding/decoding result of real multi-spectral images

The real multi-spectral images as shown in Fig. 2, copyrighted by Miyake Laboratory, Chiba University, were in 16bits 5 channels *TIFF* format.

The spectral reflectance curve of each pixel of an image $\rho_{cu}(\lambda)$ was calculated from 5 channels image data using its own multiple regression formula. Then the *CIEXYZ* and *sRGB* values were calculated from the spectral reflectance curve $\rho_{cu}(\lambda)$. The objective of *LabRGB*, here, is to encoding/decoding the above spectral reflectance curve $\rho_{cu}(\lambda)$ to obtain $\hat{\rho}(\lambda)$ with a minimum spectral and colorimetric estimation error.

Encoding is done by substituting $\rho_{cu}(\lambda)$ into Eq. 8 to obtain $b_1 \sim b_6$, substituting $b_1 \sim b_6$ into Eq. 13 and calculate *CIEXYZ and CIELAB values from* $\rho_{cu}(\lambda)$ to obtain *LabRGB* encoding values $L^*\ a^*\ b^*\ w_1\ w_2\ w_3$.

Decoding is done by Eq. 3 and Eq. 14 to obtain $w_4\ w_5\ w_6$, then substituting $w_4\ w_5\ w_6$ and the last three *LabRGB* encoding values $w_1\ w_2\ w_3$ into Eq. 2 to obtain $\hat{\rho}(\lambda)$.

The *LabRGB* encoding/decoding images were shown in Fig. 3. D50 was used in encoding/decoding. The original images in Fig. 2 and the *LabRGB* encoding/decoding images in Fig. 3 look almost the same and cannot tell the difference by human eye. The colorimetric and spectral accuracies were shown in Table 1 and Table 2 respectively. Surprisingly colorimetric and spectral estimation errors were small for all images.

Figure.4 shows the local worst area in P1 image in terms of ΔEab. More than 2 ΔE_{ab} are indicated as white color. For example, the saturated colors in right top of P1 image were more than 2 ΔE_{ab}. Therefore the encoding/decoding using illuminant D65 observed by illuminant A is the worst case in P1 image. The colorimetric accuracies show the same trend in Table 1.

Figures.5, 6 and 7 show all P1~P8 images observed by illuminant A with the encoding/decoding using illuminant D65, D50 and BBR4K respectively. Illuminant D50 and BBR4K are much better than illuminant D65, but the difference between illuminant D50 and BBR4K are not so significant. Thus, for encoding/decoding, illuminant D50 is an appropriate choice to minimize ΔE_{ab} for the local worst area.

It should be noted that we can eliminate color estimation error completely (ΔE_{ab} =0), if we choose the encoding/decoding illuminant same as the observation illuminant. It can be said by *LabRGB* definition.

Table 1. Comparison of the colorimetric estimation errors (standard deviation of the 764 x 508 pixel ΔEab in each image)

Image name	*LabRGB* encoding/decoding illuminants	Observation illuminants		
		D65	D50	A
P1	BBR4K	0.2932	0.2187	0.2748
	D50	0.1647	0	0.4028
	D65	0	0.1620	0.5296
P2	BBR4K	0.1281	0.0980	0.1228
	D50	0.0742	0	0.1722
	D65	0	0.0748	0.2289
P3	BBR4K	0.2790	0.2277	0.2877
	D50	0.1452	0	0.4156
	D65	0	0.1529	0.5343
P4	BBR4K	0.4138	0.3572	0.4667
	D50	0.2899	0	0.5702
	D65	0	0.2936	0.7871
P5	BBR4K	0.3917	0.3252	0.4186
	D50	0.2473	0	0.5490
	D65	0	0.2521	0.7401
P6	BBR4K	0.4737	0.3613	0.7141
	D50	0.4423	0	0.7505
	D65	0	0.4419	1.1115
P7	BBR4K	0.2335	0.1816	0.1771
	D50	0.1071	0	0.2705
	D65	0	0.1102	0.3476
P8	BBR4K	0.3749	0.3408	0.5382
	D50	0.2911	0	0.6627
	D65	0	0.2999	0.8872

Figure 2. The original images, copyrighted by Miyake Laboratory, Chiba University, were used in the encoding/decoding test. The original images were name as P1 ~ P8 and are located from top to bottom respectively. The pictures observed by D65, D50 and A located from left to right.

Figure 3. The images after LabRGB encoding/decoding took place. In this case, illuminant D50 was used in LabRGB encoding/decoding. The images were P1 ~ P8 located from top to bottom respectively. The pictures observed by D65, D50 and A located from left to right.

Figure 4. LabRGB encoding/decoding images P1. The pictures are for encoding/decoding using illuminants D65, D50 and A located from left to right. The pictures observed by D65, D50 and A located from top to bottom. More than 2 ΔE_{ab} are indicated as white color.

Figure 5. LabRGB encoding/decoding images P1 through P8. The pictures are for encoding/decoding using illuminant D65 observed by illuminant A. More than 2 ΔE_{ab} are indicated as white color.

Table2. Comparison of the spectral estimation errors (standard deviation of the 31 wavelength sampling points x 764 x 508 pixel $\Delta\rho$ in each image)

Image name	*LabRGB* encoding/decoding illuminants		
	BBR4K	D50	D65
P1	0.005975	0.006022	0.006036
P2	0.005935	0.005972	0.005981
P3	0.013721	0.013969	0.014044
P4	0.008509	0.008642	0.008678
P5	0.007921	0.008072	0.008114
P6	0.009485	0.009574	0.009583
P7	0.004600	0.004666	0.004686
P8	0.021393	0.021711	0.021791

Figure 6. LabRGB encoding/decoding images P1 through P8. The pictures are for encoding/decoding using illuminant D50 observed by illuminant A. More than 2 ΔE_{ab} are indicated as white color.

Figure 7. LabRGB encoding/decoding images P1 through P8. The pictures are for encoding/decoding using illuminant BBR4K observed by illuminant A. More than 2 ΔE_{ab} are indicated as white color.

Conclusion

The spectral encoding/decoding method, called *LabRGB* derivation was described in detail including fast straightforward calculation of encoding/decoding calculation. *LabRGB* was applied to 8 different types of multi-spectral images to evaluate the encoding/decoding characteristics. *LabRGB* performed well in encoding/decoding various types of multi-spectral images and confirmed to be suitable for practical use.

Future plan is to accumulate *LabRGB* test data to multi-spectral imaging systems and continue a performance evaluation.

Acknowledgements

The authors would like to express many thanks to Miyake Laboratory in Chiba University to accept using their multi-spectral images, indicated as P1 through P8, in this study.

References

[1] Fumio Nakaya and Noboru Ohta, Spectral encoding / decoding using *LabRGB*, 15th Color Imaging Conference, 190-194 (2007)

[2] M.W.Derhak, M.R.Rosen, "Spectral Colorimetry using LabPQR - An Interim Connection Space", Journal of Imaging Science and Technology, 50, pp. 53-63 (2006).

[3] CIE 15: Colorimetry, Third Edition (2004).

[4] G. Wyszecki and W. Stiles, Color Science, 2nd Edition, John Wiley & Sons (1982).

[5] S. Tsutsumi, M. R Rosen and R. S. Berns, "Spectral Color Management using Interim Connection Spaces based on Spectral Decomposition", Proc. IS&T/SID 14h Color Imaging Conference, pp. 246-251 (2006).

[6] CIE 15: Colorimetry, Third Edition (2004)

Biography

Fumio Nakaya received his B.S degree in Mechanical engineering from Keio University in Japan in 1976. Since 1976 he has worked in research and development divisions at Fuji Xerox Co., Ltd in Kanagawa, Japan. His work has primarily focused on image quality and image quality design, including microscopic image structure for high quality color image using dry toner, color management in multimedia equipment and systems. He is a member of the IS&T and the Institute of Image Information and Television Engineers.

Fumio Nakaya
Fuji Xerox Co., Ltd.
Corporate Technology Planning,
Research & Technology Group
430 Green Tech Nakai, Sakai Nakai-cho,
Ashigara Kami-gun, Kanagawa 259-0157, Japan
Tel: (011)81-465-80-2395
Fax: (011)81-465-81-8970
E-mail: fumio.nakaya@fujixerox.co.jp